Icarus 336 (2020) 113457

Contents lists available at ScienceDirect

Icarus

journal homepage: www.elsevier.com/locate/icarus

Catastrophic disruption of icy bodies with sub-surface oceans

M.J. Burchell *, K. Landers, K.H. Harriss, M.C. Price

Centre for Astrophysics and Planetary Science, School of Physical Sciences, University of Kent, Canterbury, Kent, CT2 7NH, United Kingdom

ARTICLE INFO

Keywords:
Ices
Satellites (general)
Impact processes
Europa
Enceladus

ABSTRACT

Several icy bodies in the outer Solar system have extensive internal oceans. In several bodies the oceans are believed to be so extensive they decouple the interior core from the icy surface. A major evolutionary driver in the Solar System is high speed impacts – which lead to cratering or even disruption of the target body. Here we consider how the presence of an internal ocean modifies the energy density needed to disrupt an icy body with an internal ocean. We find that in laboratory experiments on decimetre scale bodies, the energy density to cause disruption is 16.25 ± 1.35 J kg^{-1}, compared to 18.0 ± 0.7 J kg^{-1} for solid ice bodies. This suggests that for the purposes of impacts the bodies behave as if a solid with the same density. Predictions of the lifetimes of such icy bodies against impact disruption thus need not take the interior ocean into account.

1. Introduction

There are now several cases of icy bodies in the Solar System with suspected sub-surface oceans (e.g. Europa Carr et al., 1998; Pappalardo et al., 1999; Neukum et al. (1999); Sparks et al., 2016, Ganymede Kivelson et al., 2002, Callisto Khurana et al., 1998, Enceladus Nimmo et al., 2007; Cadek et al., 2016; Dougherty et al., 2006; Waite et al., 2006; Hansen et al., 2006, Pluto Hammond et al., 2016 etc.). In these bodies, tidal or interior heating, combined with the overall heat flow rates and with varying chemical compositions of the water/ice (i.e. brines, with various possible volatiles such as methane or ammonia in the ice also changing the melting point), is held to permit a liquid layer between the silicate/metallic core and the surface ice (Sohl et al., 2010; Grasset et al., 2017). Like all Solar System bodies, these objects are subject to high speed impacts which can result in cratering or disruption (Zahnle et al., 2003). However, the presence of an interior liquid layer (or subsurface ocean) may influence the outcome of such impacts. Here we report on how a body with a solid water ice surface and a liquid water interior responds to a severe impact. We do this by impacting model ice spheres with water interiors in the laboratory using high speed projectiles. The surface ice layer thickness was approximately 25% of the overall target diameter.

High speed impacts are typical evolutionary processes in the Solar System e.g. Osinski and Pierazzo (2013). Given the high speed of such events (typically in excess of a km s^{-1}), the materials involved are shocked to extreme pressures (10–100 s of GPa) and respond as if they lack shear strength – such processes are therefore called hydrodynamic. Possible outcomes range from cratering to catastrophic disruption of the target body. If disrupted, the fragments of the target may disperse or re-accumulate under self-gravity (if the target is sufficiently large) to form a rubble pile body. Studies of impacts and catastrophic disruption include computer simulations (e.g. Benz and Asphaug, 1999; Leinhardt and Stewart, 2012; Cox and Bauer, 2015), development of analytic models (e.g. Leliwa-Kopystynski et al., 2016), and laboratory studies in impact facilities at small (cm) scale such as (Ryan et al., 1999; Leliwa-Kopystynski et al., 2008; Michikami et al., 2016; Morris and Burchell, 2017). All these types of study provide insights into the underlying processes of disruption. The recognition of sub-surface oceans on some icy satellites in the outer Solar System, introduces a new element to understanding impact processes: a liquid subsurface layer may well not only cause behaviour very differently to that of homogenous solids, but also to those cases where layering involves a solid substrate such as ice directly on top of rock. The presence of a liquid interior may thus well influence the impact process in a novel ways.

Hydrocode modelling of impacts on icy bodies with liquid interiors has been used to predict the thickness of the Europan ice (in excess of 3–4 km (Turtle and Pierazzo, 2001), or around 7 km (Bray et al., 2014). Other simulations suggest that even for Europan surface ice thicknesses up to 40 km, the ice would be penetrated by an impact at least every 250 *My* (Cox and Bauer, 2015). Such simulations have also been performed on other bodies such as Enceladus, e.g. Monteux et al. (2016) which assesses how impactors can penetrate the icy shell and influence the shape of the interior core. As well as for cratering, simulations have been run for catastrophic disruption of purely icy bodies. For example, it has

* Corresponding author.
E-mail address: m.j.burchell@kent.ac.uk (M.J. Burchell).

https://doi.org/10.1016/j.icarus.2019.113457
Received 21 February 2019; Received in revised form 12 July 2019; Accepted 27 September 2019
Available online 29 September 2019

been shown that icy bodies are disrupted more easily than rocky bodies of similar size (Benz and Asphaug, 1999). Analytic models also exist and can be used to predict the catastrophic disruption limit for a body made purely of ice, e.g. Leliwa-Kopystynski et al. (2016). However, these models have not been run for ice surfaces over liquid interiors.

Laboratory experiments at mm or cm size scales also provide useful insights. For example, impacts in semi-infinite ice at cm scales (Leliwa-Kopystynski et al., 2008) have been compared with impacts in ice layers over various substrates such as water or clay (Greeley et al., 1982), or water, sand and basalt (Harriss and Burchell, 2017). This can alter crater size, with crater diameter decreasing as ice thickness decreased and the crater punches through into the subsurface material. For relatively very thin ice layers, although the presence of a substrate is important, the nature of the subsurface has little influence on growth of the hole (crater) in the ice, with the exception of spall, where a subsurface of basalt has been shown to create a larger spall diameter then that observed in impact into ice over water and sand. Conversely, for relatively thick ice, which fully contains the impact crater, there is no influence at all of the presence of a substrate on the outcome of the impact. However, for intermediate ice thicknesses (some 7 to 15½ times the projectile diameter in (Harriss and Burchell, 2017)), both the presence of the substrate and its composition can influence the outcome of the impact.

This leaves open the question of what happens in catastrophic disruption of icy bodies with interior liquid layers (i.e. oceans). Accordingly we have investigated impacts on ice spheres with a water interior.

2. Method

The experiments were performed using a two stage light gas gun at the Univ. of Kent (Burchell et al., 1999). The targets were spheres 16–18 cm in diameter, with a surface ice layer 4 cm thick and a liquid water interior. The targets thus had a thick ice shell equivalent to 25% of the target radius. Ten shots were carried out (see Table 1). The projectiles were 1.5 mm dia. glass spheres, impacting at speeds from 1.5 to 5.56 km s^{-1}. A high-speed video camera and an Ultra-8 high speed camera were used to image the impacts.

The ice targets used in this work were made using purified water which had been boiled to drive off dissolved gases. The water was then rapidly cooled by running liquid water over the exterior of its container, and then packing the container in crushed ice. The water was then pumped into a pre-inflated rubber balloon. The water filled balloon was then placed in a spherical mould (made of two insulated hemispheres) to shape it and placed in an upright freezer (set to −25 °C) for 24 h. The slow freezing process caused a clear ice shell to form containing an inner liquid core. The thickness of this ice layer was controllable by varying the time spent in the freezer: 24 h was found to produce a 4 cm thick ice shell for a target diameter of 17 cm.

For impacts, targets were placed in the target chamber of the Kent two stage light gas gun (Burchell et al., 1999). The chamber was evacuated to 50 mbar during a shot, so that the projectile was not decelerated after being launched from the barrel of the gun. Typical pump down times were 15–20 min from when the target was placed in the chamber to when the gun was fired. The sabot used to launch the projectile was discarded in flight and its components did not reach the target chamber. The projectile speed was measured at two laser stations along its flight path, with an uncertainty of less than ±1%. All impacts were at normal (or near normal) incidence. Note that the gun fires horizontally, and all shots were aimed at the equator of the targets, but there is a slight spread in impact points of up to around ±½ cm. Post shot the targets were removed from the gun typically 10 min after the impact occurred.

The craters produced in this work are relatively large compared to the size of the target body, and are influenced by the spherical nature of the target surface. In a typical shot, the crater thus usually has a nearly flat surface extending laterally across the sphere to its edges, and with a deeper central pit, similar to that described in Leliwa-Kopystynski et al. (2008).

After a shot the target was immediately removed from the target chamber and weighed. Any ice ejecta or target fragments were also removed and weighed. If water escaped from the target during a shot it was captured in trays beneath the target and also weighed after the shot. Impact crater diameters were measured directly on the ice target and the values presented are the result of an average over several (usually 4) individual diameters on the same crater. In many shots a deeper, and more heavily damaged central pit was observed in the crater. The diameter of this inner pit was also measured. The crater depth was measured via a two-step process. After a shot, if the sphere was still intact, it was placed beneath a horizontal measuring station with the crater at the top of the target. A depth profile was then obtained across the crater and the depth of the centre of the crater below the surviving ice surface was found. However, the true depth is that below the original ice surface which was removed in the cratering process. If we assume the roughly flat ice surface exposed by the impact represents a chord across a circle (taking a cross-section through the sphere), then the sagitta above this chord has to be added to depth of the central pit observed in crater. This sagitta is found by geometry, knowing the crater diameter (the chord) and the original sphere diameter. The crater volume is found by the reduction in mass of the target pre and post- shot. In cases where interior water escaped through fractures in the ice sphere, this was captured in the trays beneath the target and not included in crater volume.

Two other parameters are given in Table 1. The first is Q, the energy density in the impact. This is obtained from the projectile energy divided by the target mass pre-impact. The second derived parameter, is the mass of the largest target fragment post shot, normalized to the total target mass pre-impact. For non-disrupted targets, this is also the mass of the target itself (ice shell plus water interior) minus the mass of the material ejected from the crater. When the targets were fully disrupted, the largest fragment is the largest surviving piece of ice from the shell.

Table 1
Details of the shots in this work.

Impact speed (km s^{-1})	Impact energy density Q (J kg^{-1})	Crater total dia. (mm) ±0.1	Inner crater pit dia. (mm) ±0.1	Crater depth (mm) ±0.1	Crater volume (cm^3)	Mass largest fragment normalised to target mass	Impact outcome
1.50	1.68	48.9	7.2	12.9	15.0	0.9995	Crater
2.27	3.86	73.2	17.3	16.9	34.2	0.9988	Crater
2.84	6.04	61.96	20.0	17.1	63.3	0.9977	Crater
3.13	6.78	62.4	32.2	n/a	105.0	0.9975	Crater
3.01	7.24	85.1	n/a	20.5	75.0	0.9964	Crater
3.46	8.86	80.1	42.1	18.2	128.4	0.9957	Crater
4.17	13.0	117.3	34.1	n/a[a]	445.5	0.9849	Penetrating crater
4.46	14.9	80.2	43.0	24.9	539.9	0.9305	Crater
4.85	17.6	n/a	n/a	n/a	n/a	0.1260	Disruption
5.56	25.5	n/a	n/a	n/a	n/a	0.2342	Disruption

[a] In this case the ice shell was penetrated but not disrupted, so the total crater depth is unknown as it may have formed a transient crater in the water beneath the ice.

We measured in detail the mass of the largest ejected fragments post-impact in five of the shots. For non-disrupted targets, the large fragment was the original body and the smaller masses from the largest pieces of ice ejected from the crater. For a disrupted event, the fragments were from the broken ice shell itself.

3. Results

The sequence of how an impact progresses from cratering in the ice shell, to penetrating the shell (but leaving it otherwise intact), to complete disruption of the ice is shown in Figs. 1–3, at increasing impact speeds 3.01, 4.17 and 4.85 km s^{-1}, corresponding to impact energy densities (Q) of 7.24, 13.0 and 17.6 J kg^{-1} respectively. The sequence of images in Fig. 1 shows a non-penetrating impact in the surface ice (3.01 km s^{-1}). Lower speed impacts produced fewer concentric fractures and more radial ones originating at the crater. At around 3.0 km s^{-1}, damage is confined to the region of the sphere closest to the impact point, although individual fractures do penetrate from top to bottom of the ice layer. Fig. 2 shows the hole made in an impact at 4.17 km s^{-1}, which penetrated the ice shell, but left the rest of the shell intact (albeit heavily fractured). The hole is equivalent to removal of 1% of the surface area of the ice sphere (some 513 times the cross sectional area of the projectile). At 4.17 km s^{-1}, although the fracturing is extensive and penetration occurs, there are still significant regions of clear ice in the ice layer (i.e., with little macroscopic fracturing), particularly in the rearward hemisphere of the ice. At around 4.85 km s^{-1} the ice is heavily fractured across the whole body and ice shell integrity fails. In Fig. 3, the high speed camera shows a series of images during a penetrative impact at 4.85 km s^{-1}. Unlike the impact at 3.01 km s^{-1} (Fig. 1) the fracturing is more extensive in the forward hemisphere (as seen from the impact point) and also extends heavily into the rearward hemisphere. The onset of breaking apart of the surface thus occurs once fracturing extends across the whole body.

The measurements of the crater dimensions are given in Fig. 4. It appears that the maximum crater diameter a sphere can sustain is approximately 0.6 times the sphere diameter. This compares to a value of 0.82 found for solid ice spheres of similar size (Leliwa-Kopystynski et al., 2008). The maximum crater depth which can be sustained in the surface ice layer before penetration occurs is 0.6 times the ice thickness. It has been suggested from modelling (Cox and Bauer, 2015), that breach of the ice surface occurs when transient crater depth exceeds 0.9 times the ice shell thickness. However, the models are for planetary scale impacts not the decimetre laboratory scale here.

The mass of the largest fragment mass is shown in Fig. 5a. This gives the catastrophic disruption energy density (Q^*, defined as the value of Q for which the largest intact fragment has 50% of the original mass) as being in the range 16.25 ± 1.35 J kg^{-1}. In earlier work on solid ice spheres of similar size and at similar impact speeds (where disruption occurred at about 5 km s^{-1}), Q^* was found to be 18.0 ± 0.7 J kg^{-1} (Leliwa-Kopystynski et al., 2008), very similar to that found here when a liquid interior was present. Note however, that these values are some 50 times smaller than predicted by hydrocode modelling for impacts on decimetre scale solid ice targets (Benz and Asphaug, 1999), and are at the very low end of the range predicted in analytic modelling (Leliwa-Kopystynski et al., 2016).

Fig. 2. Face on view of a target after a shot at 4.17 km s^{-1}. The impact crater is seen as a hole in the ice layer. The ice shell itself survived the impact intact, but was heavily fractured. Some of the fractures appeared to penetrate through the whole ice shell from surface to interior.

Looking at the fragment size distribution (Fig. 5b), the behaviour of the cumulative size distribution of the largest fragments moves from a concave to a convex shape (in log-log space) as one goes from sub-critical to critical disruption. This is similar to that reported elsewhere as one goes from sub-critical to critical disruption in a variety of scenarios, e.g. in modelling (Durda et al., 2007), observations of asteroid family members (Leliwa-Kopystynski et al., 2009) and laboratory impact experiments (Morris and Burchell, 2017).

4. Discussion

Disruption of the target occurs when fracturing has spread around the whole ice layer. In general, solid, homogeneous brittle spheres fail in a variety of ways. Small spheres impacted at low speed undergo meridianal fracturing. As the size of the sphere and degree of damage increase, a Hertzian cone fracture appears at the impact point, and fractures spread in the near surface around the impact point. These spread laterally and rise up at their ends to intercept the surface, lifting petal-like plates away from the sphere. As the degree of damage increases, these fractures penetrate further through the sphere leaving a central core intact beneath the crater, or a cone like largest fragment extending from beneath the impact site to the rear surface. Finally, when the energy density is high enough, the whole body breaks into multiple small fragments. This is shown for glass in Gorham and Salman (2005) and ice (Ryan et al., 1999). This is expanded on for basalt targets

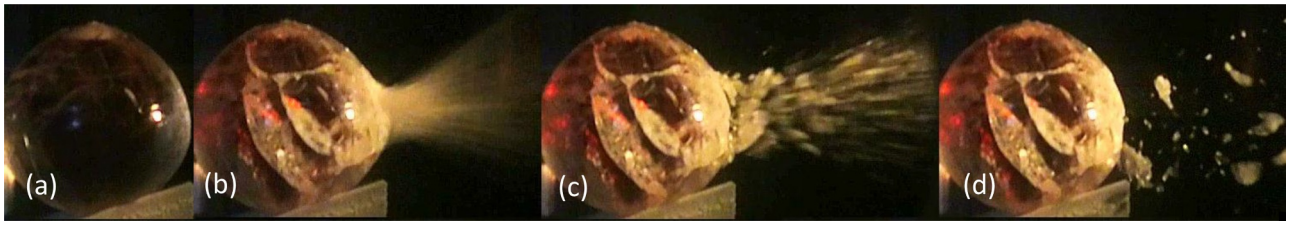

Fig. 1. A target during impact at 3.01 km s^{-1}. (a) Pre-impact. (b)–(d) During the impact. The impact was horizontal from the right and each image is separated by 15 ms. In (b) the classic cone shaped ejecta cloud of fine material has formed at the impact site, and fractures have already formed over the leading hemisphere of the target (as seen from the impact point). There are both concentric fractures and radial ones emanating from the impact site. In (c) and (d) larger, slower ejecta are removed from the impact site, but no further large scale fracturing occurs. The ice surface layer was not penetrated at the impact point. However, subsequent examination showed that a few % of the interior water had been lost, possibly through the concentric fractures, some of which reached the interior. These penetrating fractures were in isolated regions and did not link up across the whole shell.

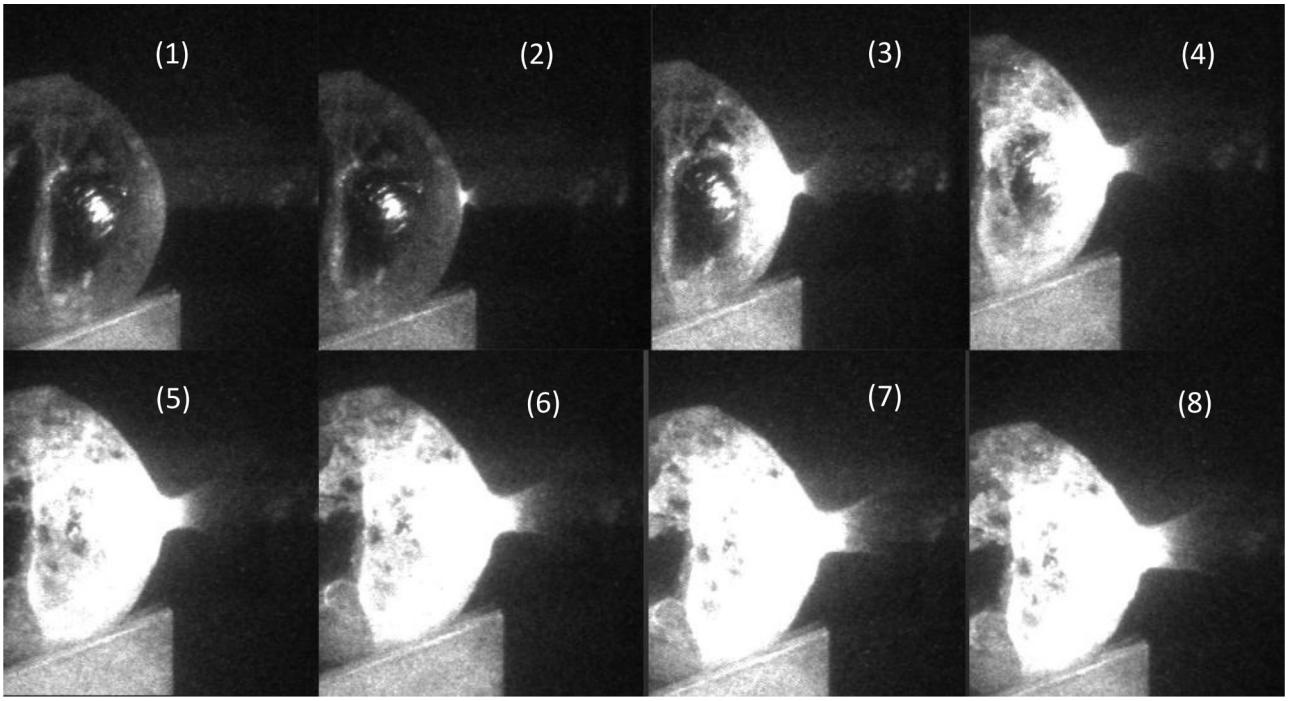

Fig. 3. Eight images taken during an impact at 4.85 km s^{-1}. Each frame is separated by 0.1 ms. The impact was horizontal from the right and occurred between the first and second frames. ½ of the leading hemisphere is heavily fractured by frame 3, with the whole leading hemisphere showing fracturing by frame 4, suggesting the fractured region has spread at around 667 m s^{-1}. Also, whilst fractured, the sphere has not begun to dis-assemble during the first 0.6 ms after impact.

undergoing impact in Michikami et al. (2016), where four degrees of impact damage are given: Type I – just a crater, Type II – fracturing extends to sides of the target, Type III – the largest fragment remaining is an exposed core, and Type IV – complete disruption into multiple small fragments. An example for a cement target which is Type III/IV is shown in Morris et al. (2013). These however are for brittle, homogeneous bodies.

In the case here, there are two complications: there is a boundary between the surface (ice) and interior (water), and the interior is a non-brittle material which will not undergo fracture as the surface does. Either of these differences can reasonably be held to change the outcome of a catastrophic disruption event, particularly as it has previously been shown that impacts in ice over differing substrates can influence the outcome of the impact. Yet, remarkably, we find that here the Q^* value has not measurably changed compared to a solid, homogeneous ice target.

The experimental results presented here for an ice surface over a deep internal ocean, span the range; cratering (a local effect); surface layer breach (again local, but with damage to the ice layer extending to far larger regions of the body); and catastrophic disruption (global damage to the ice surface removing its structural integrity). Note that in bodies at >10–100 s of km scales, not only will the strength related properties of the body be scale dependent, but the broken body will also have to disperse against self-gravity, else it can re-accumulate. Unless the target material is expelled at above local escape velocity, the loss of the structural integrity of the ice surface will not lead to a large degree of mass loss. It will however redistribute the liquid interior over the original surface.

Another critical issue in disruption of an icy body with a liquid water interior, is what happens to the water? For solid bodies, the displaced material fragments or vaporizes and these discrete pieces and vapour start to move apart. The material may then reassemble under self-gravity or escape. The novelty here is that we have a process in which significant amounts of material, i.e. the liquid water, has no internal strength at any stage of the impact/disruption process, even during the dispersal and reassembly period. Further it may undergo a phase-transition, i.e. freeze, during this time and thus start to behave as a collection of solid fragments. Note that this is different from plumes emitted from an internal ocean, where fine sprays are ejected and likely to freeze rapidly. Here significant liquid material is expelled simultaneously and this should be considered. Vaporisation of significant amounts of the displaced material may not occur unless the impact speed was high (above 8 km s^{-1} Movshovitz et al., 2015) so is unlikely if the impactor on an icy satellite was co-orbiting the parent planet. Such speeds can be reached however, if the impactor falls into say a Jovian or Saturnian system from elsewhere in the Solar System, particular if the impact is on an inner satellite.

There is evidence from various icy satellites that surface penetration has occurred on such bodies in the past. On Europa, the Tyre and Callanish multi-ring basins are held to represent areas where breach of the ice surface has been achieved without catastrophic disruption occurring (Kadel et al., 2000; Moore et al., 2001). The lack of wider scale break-up of the ice surface around these sites suggests the breach was marginally achieved. Taking the radius of these basins as 40–50 km, suggests each site represents some 1.6 to 2.5% of the Europan surface, comparable to the 1% found here for a non-catastrophic breach at 4.17 km s^{-1}. Fuller breaches of ice surface layers on real bodies may not result in recognizable impact craters, but rather in regions of chaotic terrain (Cox et al., 2008).

There has been interest in impacts on water bearing bodies such as the Earth. For smaller impacts (which produce local cratering in the water layer and possibly in the ocean floor beneath) if the impact is into water there are three roughly equal paths for the water: ejection into the stratosphere (where it may remain for long periods), vertical removal in a crown around the impact (which then falls back causing local damage), and lateral flow away from the impact site e.g. see Sonett et al. (1991) and Gisler et al. (2003, 2011). How the water interacts with the projectile is discussed in detail in Davison and Collins (2007). There may also be submarine craters formed, e.g. see Dypvik et al. (2003) for a review. Modelling suggests submarine craters will be found if the water cover is less than 5–7 times the projectile diameter (Gisler et al., 2011), or 8 times projectile diameter (Davison and Collins, 2007), whereas

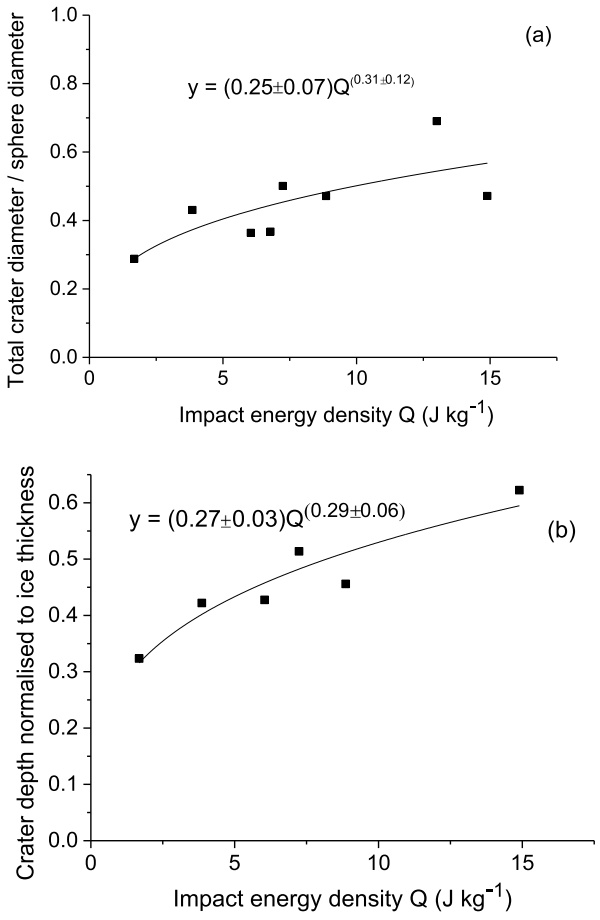

Fig. 4. Crater dimensions vs. impact energy density for non-disruptive impacts. (a) Total crater diameter normalised to target diameter. (b) Crater depth normalised to ice thickness. The fit shown in (a) is of exponential form, suggesting a slowing of the increase in crater diameter as the disruption limit was approached. For an ice thickness of 4 cm, the maximum crater diameter without exposing the liquid interior would have been 10.2 cm, or some 0.6 times target diameter. The shot at 13 J kg^{-1} (4.17 km s^{-1}) just exceeds this limit and thus penetrated the ice shell, without disrupting the total body. In (b) the crater depth exponentially grows to some 60% of ice thickness before disruption occurs. The exception is for the shot at 13 J kg^{-1} where the total crater depth is unknown but exceeds 100% of ice thickness, i.e. the ice layer was penetrated.

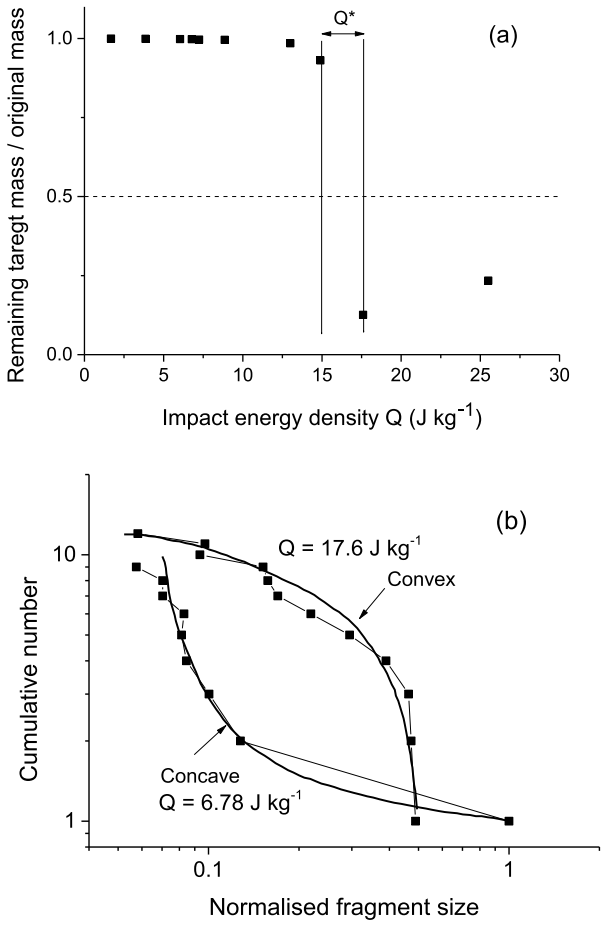

Fig. 5. (a) Surviving intact largest mass post-shot (normalised to total pre-impact mass) vs. impact energy density Q. There is a sudden failure of the targets between $Q = 14.9$ and 17.6 J kg^{-1} (marked by vertical lines). The catastrophic energy density is defined as that which produces a surviving largest mass fraction of 0.5 (shown by a dotted horizontal line), and in this case thus lies between 14.9 and 17.6 J kg^{-1}. (b) The size-frequency distribution (SFD) for a non-disruptive impact ($Q = 6.78$ J kg^{-1}, $v = 3.31$ km s^{-1}) and a catastrophically disrupting impact ($Q = 17.6$ J kg^{-1}, $v = 4.85$ km s^{-1}). The heavy solid lines show the general behavior of the SFD in each case (convex vs. concave in log-log space). For the sub-critical impact it is concave, whereas in the catastrophic case it is convex.

laboratory experiments suggest the cut-off is 10 or more times the projectile diameter (Gault and Sonnet, 1982; Baldwin et al., 2007; Milner et al., 2008). Given that the simulations and experiments were performed over a wide range of speeds (5–15 km s^{-1}), and projectile sizes (mm to km scale) and compositions (granite to steel), this is a surprisingly narrow range of normalized water depths. This is important, because whilst sub-critical impacts may not completely disrupt the body, they can cause deformation of the rocky core of a layered body beneath the liquid layer. In the case of icy satellites, the impactor has to penetrate the surface ice first. This has been modelled for small bodies such as Enceladus (Monteux et al., 2016) where it was found that the presence of a liquid ocean (with no shear strength) between the icy mantle and rocky core, reduces damage to the core but can increase the disruption of the icy mantle. It would be interesting to test this in the laboratory, but that is for future work.

Large scale terrestrial impacts often focus on mass extinction events or the moon forming event (Canup and Asphaug, 2001). In the latter case, they assume the event is so violent the presence of a thin surface water layer can be ignored (or in models for a hot target pre-impact, was not present). These models however, assume impacts on a larger body (the Earth) with relatively less water (estimates for the volume of water on Enceladus for example range up to 40% of the total mass of the body Cadek et al., 2016) so do not provide a guide to what happens to the water displaced from sub-surface oceans on icy bodies. The particular issue there is how the ice surface constrains the motion of water as it moves away from the impact site. The resulting interior pressures may enhance the disruption of the icy surface. And at the impact site the surrounding ice may be further damaged by the fall under gravity of a crown of ejected water at the impact point. In our study we have a relatively thick ice layer, this issue may be more acute with a thinner ice layer.

If the target body were a pure waterworld, it is often assumed that the consequence of an impact would be a large tsunamis. However, recently it has been felt that the waves these impacts produce are unlike traditional tsunamis and do not propagate so well (Gisler et al., 2011). Here however, there is the additional constraint that any bulk movement of water is restricted by the presence of the overlaying ice. The failure of that ice layer may thus be a result of both propagation of shock waves through the ice, combined with an internal overpressure caused by shock waves in the water. Again, the thickness of the ice may be critical.

Another way an internal ocean can influence the outcome of an impact can be illustrated by considering Pluto. An impact on Pluto has

been suggested for the origin of Pluto's satellite Chiron (Canup, 2011), with the model for the pre-impact Pluto supposing an ice surface which directly overlays a rock-ice interior. A sub-surface ocean on Pluto has however also been suggested, e.g. Hammond et al. (2016), and its influence on this process is unclear. Such an ocean would likely not be pure water, but have mixtures of materials such as ammonia in it (which would act as an antifreeze) which may well differ from those in the ice rich surface mantle (e.g. see Desch, 2015 for a discussion). Whilst small amounts of materials like ammonia in the surface ice, are not likely to influence the impact process (Grey and Burchell, 2004), any satellites that form after the impact may contain compositional signatures dependent on whether they formed with contributions from the icy mantle or with significant amounts of the liquid interior ocean. The fate of an interior ocean after a disruptive impact and the signature it may leave on the debris from the event is thus still unclear.

5. Conclusions

Impacts on icy satellites have been modelled previously, but usually in terms of what is needed to penetrate the crust, (e.g. Turtle and Pierazzo, 2001). Here we have carried out experiments concerning disruption. Disruption occurs after the resultant crater is of sufficient depth to penetrate the ice layer, and when fracturing of the ice has extended around the whole body. We find that, for relatively thick ice surface layers, such bodies are just as resistant to disruption as solid ice targets of similar size.

Considering physical examples in the Solar System, Europa has a relatively thin ice crust. If we take the radius of Europa as around 1560 km, then an ice shell at least 3–4 km thick (Turtle and Pierazzo, 2001), 7 km thick (Bray et al., 2014), or 8–13 km thick (Cox and Bauer, 2015), suggests the ice is 0.2–0.8% of the radius of the body. This is different for Enceladus however. Estimates of the thickness of its ice shell range include 18–22 km (Cadek et al., 2016), 21–26 km (Thomas et al., 2016), or 50–90 km (Monteux et al., 2016) which combined with a mean radius of some 252.1 km (Thomas et al., 2007) suggests the icy mantle could be some 7–36% of the radius of the body. Therefore, the work here, for bodies with relatively thick icy surfaces (some 25% of the radius of the body) is more likely to be representative of an Enceladus-like body than an Europan one.

Generalising this result for thin ice shells would clearly be interesting. Another effect not considered here is the influence on disruption of the presence of a central rocky/metallic core beneath the subsurface ocean, this still awaits experimental investigation. We also note that these results are obtained at laboratory scale in the strength regime, rather than a gravity regime applicable to bodies at 100 s of km scales. Therefore the Q^* value reported herein is the strength-dominated value at the given size scale (10 s of cm). Solar system bodies will be at larger sizes, and not only should the Q^* value be scaled as size increases, the contribution which describes the dispersal against self-gravity comes to dominate and that has not been investigated here. The development of a model which scales Q^* for such a body from the strength into the gravity dominated regime would be useful.

Other effects also need to be considered. The data here are for normal incidence impacts, whereas real Solar System impacts are typically at 45° incidence. Non-normal impacts are held to be less effective at cratering, due to a reduced coupling of the projectiles energy/momentum into the target (see for example Pierazzo and Melosh, 2000). The change in cratering efficiency in ice with impact angle has been explored experimentally (Grey et al., 2002). There it was shown that whilst crater volume and depth fall as soon as the impact angle falls from normal incidence, the crater diameter does not vary until the incidence is over 55° from the vertical. The role of the ice temperature can also be important. In the strength dominated regime, Grey and Burchell, 2003, have shown that over a wide temperature range (150–260 K crater diameter does not depend on ice temperature, but below 150 K it rises as the target ice temperature is lowered. By contrast, crater depth falls continually as ice temperature is lowered over the range 100–260 K. This suggests that in colder bodies, the surface ice layer is less likely to be penetrated. However, it should be recalled that in real examples, there will be a thermal gradient in the ice, from a relatively warmer interior surface to a cooler exterior surface layer, complicating matters further.

With these caveats, the results suggest that in calculations of lifetimes of icy bodies against impacts, the presence of an internal ocean can be ignored, and the body treated as a solid ice body of equal density. That is, the presence of the ocean does not change the overall outcome of a catastrophic impact event. This is important, it implies for example, that the modelling of catastrophic disruption at large scales based on pure ice bodies remains valid (e.g. Movshovitz et al., 2015).

Acknowledgements

The experiments reported here were performed at the University of Kent supported by STFC grants ST/K000888/1 and ST/N000854/1. The light gas gun was operated by M. Cole.

Supplementary materials

Supplementary material associated with this article can be found, in the online version, at doi:10.1016/j.icarus.2019.113457.

References

Baldwin, E.C., Milner, D.J., Burchell, M.J., Crawford, I.A., 2007. Laboratory impacts into dry and wet sandstone with and without an overlying water layer: Implications for scaling laws and projectile survivability. Meteorit. Planet. Sci. 42, 1905–1914.

Benz, W., Asphaug, E., 1999. Catastrophic disruptions revisited. Icarus 142, 5–20.

Bray, V.J., Collins, G.S., Morgan, J.V., Melosh, H.J., Schenk, P.M., 2014. Hydrocode simulation of Ganymede and Europa cratering trends - how thick is Europa's crust? Icarus 231, 394–406.

Burchell, M.J., Cole, M.J., McDonnell, J.A.M., Zarnecki, J.C., 1999. Hypervelocity impact studies using the 2 MV Van de Graaff dust accelerator and two stage light gas gun of the University of Kent at Canterbury. Meas. Sci. Techol. 10, 41–50.

Cadek, O., Tobie, G., Van Hoolst, T., Masse, M., Choblet, G., Lefevre, A., Mitri, G., Baland, R.M., Behounkova, M., Bourgeois, O., Trinh, A., 2016. Enceladus's internal ocean and ice shell constrained from Cassini gravity, shape, and libration data. Geophys. Res. Lett. 43 (11), 5653–5660.

Canup, R.M., Asphaug, E., 2001. Origin of the Moon in a giant impact near the end of the Earth's formation. Nature 412, 708–712.

Canup, R.M., 2011. On a giant impact origin of Charon, Nix, and Hydra. Astron. J. 141, 35–43.

Carr, M.H., Belton, M.J.S., Chapman, C.R., Davies, A.S., Geissler, P., Greenberg, R., McEwen, A.S., Tufts, B.R., Greeley, R., Sullivan, R., Head, J.W., Pappalardo, R.T., Klaasen, K.P., Johnson, T.V., Kaufman, J., Senske, D., Moore, J., Neukum, G., Schubert, G., Burns, J.A., Thomas, P.C., Veverka, J., 1998. Evidence for a subsurface ocean on Europa. Nature 391 (6665), 363–365.

Cox, R., Ong, L.C.F., Arakawa, M., Scheider, K.C., 2008. Impact penetration of Europa's ice crust as a mechanism for formation of chaos terrain. Meteorit. Planet. Sci. 43, 2027–2048.

Cox, R., Bauer, A.W., 2015. Impact breaching of Europa's ice: constraints from numerical modelling. J. Geophys. Res. Planets 120, 1708–1719. https://doi.org/10.1002/2015JE004877.

Davison, T., Collins, G.S., 2007. The effect of the oceans on the terrestrial crater size-frequency distribution: insight from numerical modeling. Meteorit. Planet. Sci. 42, 1915–1927.

Desch, S.J., 2015. Density of Charon formed from a disk generated by the impact of partially differentiated bodies. Icarus 246, 37–47.

Dougherty, M.K., Khurana, K.K., Neubauer, F.M., Russell, C.T., Saur, J., Leisner, J.S., Burton, M.E., 2006. Identification of a dynamic atmosphere at Enceladus with the Cassini magnetometer. Science 311 (5766), 1406–1409.

Durda, D.D., Bottke Jr., W.F., Nesvorný, D., Enke, B.L., Merline, W.J., Asphaug, E., Richardson, D.C., 2007. Size-frequency distributions of fragments from SPH/N-body simulations of asteroid impacts: comparison with observed asteroid families. Icarus 186, 498–516.

Dypvik, H., Burchell, M.J., Claeys, P., 2003. Impacts in marine and icy environments. In: Dypvik, Burchell, Claeys (Eds.), Cratering in Marine Environments and on Ice. Springer, pp. 1–20.

Gault, D.E., Sonnet, C.P., 1982. Laboratory simulation of Pelagic asteroid impact; atmospheric injection, benthic topology, and the surface wave radiation field. In: Silver, L.T., Schultz, P.H. (Eds.), Geological Implications of Impacts of Large Asteroids and Comets on the Earth. GSA Special Paper #190.

Gisler, G., Weaver, R., Gittings, M., Mader, C., 2003. Two- and three-dimensional asteroid ocean impact simulations. Int. J. Impact Eng. 29, 283–291.

Gisler, G., Weaver, R., Gittings, M., 2011. Calculations of asteroid impacts into deep and shallow water. Pure Appl. Geophys. 168, 1187–1198.
Gorham, D.A., Salman, A.D., 2005. The failure of spherical particles under impact. Wear 258, 580–587.
Grasset, O., Castillo-Rogez, J., Guillot, T., Fletcher, L.N., Tosi, F., 2017. Water and volatiles in the outer solar system. Space Sci. Rev. 212, 835–875.
Grey, I.D.S., Burchell, M.J., Shrine, N.R.G., 2002. Scaling of hypervelocity impact craters in ice with impact angle. J. Geophys. Res. E. 107 (E10), 5076. https://doi.org/10.1029/2001JE001525.
Grey, I.D.S, Burchell, M.J., 2003. Hypervelocity impact cratering on water ice targets at temperatures ranging from 100 K to 253 K. J. Geophys. Res E 108 (E3), 5019. https://doi.org/10.1029/2002JE001899.
Grey, I.D.S., Burchell, M.J., 2004. Hypervelocity impact craters in ammonia rich ice. Icarus 168, 467–474.
Greeley, R., Fink, J.H., Gault, D.E, Guest, J.E., 1982. Experimental simulation of impact cratering on icy satellites. In: Morrison, D.M. (Ed.), Satellites of Jupiter. Univ. of Arizona Press, Tucson, pp. 340–378.
Hammond, N.P., Barr, A.C., Parmentier, E.M., 2016. Recent tectonic activity on pluto driven by phase changes in the ice shell. Geophys. Res. Lett. 43, 6775–6782.
Hansen, C., Esposito, L., Stewart, A.I.F., Colwell, J., Hendrix, A., Pryor, W., Shemansky, D., West, R., 2006. Enceladus' water vapor plume. Science 311 (5766), 1422–1426.
Harriss, K.H., Burchell, M.J., 2017. Hypervelocity impacts into ice topped layered targets: investigating the effects of ice crust thickness and subsurface density on crater morphology. Meteorit. Planet. Sci. 52, 1505–1522.
Kadel, S.D., Chuang, F.C., Greeley, R., Moore, J.M., Team, G.S., 2000. Geological history of the Tyre region of Europa: a regional perspective on Europan surface features and ice thickness. J. Geophys. Res. 105, 22657–22669.
Khurana, K.K., Kivelson, M.G., Stevenson, D.J., Schubert, G., Russell, C.T., Walker, R.J., Polanskey, C., 1998. Induced magnetic fields as evidence for subsurface oceans in Europa and Callisto. Nature 395 (6704), 777–780.
Kivelson, G., Khurana, K.K., Volwerk, M., 2002. The permanent and inductive magnetic moments of Ganymede. Icarus 157, 507–522.
Leinhardt, Z.M., Stewart, S.T., 2012. Collisions between gravity-dominated bodies. I. Outcome regimes and scaling laws. Astrophys. J. 745, 79 (27 pp).
Leliwa-Kopystynski, J., Burchell, M.J., Lowen, D., 2008. Impact cratering and break up of the small bodies of the Solar System. Icarus 195 (2), 17–826.
Leliwa-Kopystynski, J., Burchell, M.J., Włodarczyk, I., 2009. The impact origin of Eunomia and Themis families. Meteorit. Planet. Sci. 44 (12), 1929–1936.
Leliwa-Kopystyński, J., Włodarczyk, I., Burchell, M.J., 2016. Analytical model of impact disruption of satellites and asteroids. Icarus 268, 266–280.
Michikami, T., Haegermann, A., Kadokawa, T., Yoshida, A., Shimada, A., Hasegawa, S., Tsuchiyama, A., 2016. Fragment shapes in impact experiments ranging from cratering to catastrophic disruption. Icarus 264, 316–330.
Milner, D.J., Baldwin, E.C., Burchell, M.J., 2008. Laboratory investigations of marine impact events: factors influencing crater formation and projectile survivability. Meteorit. Planet. Sci. 43, 2015–2026.
Monteux, J., Collins, G.S., Tobie, G., Choblet, G., 2016. Consequences of large impacts on Enceladus' core shape. Icarus 264, 300–310.
Moore, J.M., Asphaug, E., Belton, M.J.S., Bierhaus, B., Breneman, H.H., Brooks, S.M., Chapman, C.R., Chuang, F.C., Collins, G.C., Giese, B., Greeley, R., Head, J.W., Kadel, S., Klaasen, K.P., Klemaszewski, J.E., Magee, K.P., Moreau, J., Morrison, D., Neukum, G., Pappalardo, R.T., Phillips, C.D., Schenk, P.M., Senske, D.A., Sullivan, R. J., Turtle, E.P., Williams, K.K., 2001. ...MoreImpact features on Europa: results of the Galileo Europa Mission (GEM). Icarus 151, 93–111.
Morris, A.J.W., Burchell, M.J., 2017. Laboratory tests of catastrophic disruption of rotating bodies. Icarus 296, 91–98.
Morris, A.J.W., Price, M.C., Burchell, M.J., 2013. Is the large crater on asteroid (2867) Steins really an impact crater? Astrophys. J. Lett. 774, L11.
Movshovitz, N., Nimmo, F., Korycansky, D.G., Asphaug, E., Owen, J.M., 2015. Disruption and reaccretion of midsized moons during an outer solar system Late Heavy Bombardment. Geophys. Res. Lett. 42, 256–263.
Neukum, G., Phillips, C.B., Prockter, L.M., Schubert, G., Senske, D.A., Sullivan, R.J., Tufts, B.R., Turtle, E.P., Wagner, R., Williams, K.K., 1999. Does Europa have a subsurface ocean? Evaluation of the geological evidence. J. Geophys. Res.-Planets 104 (E10), 24015–24055.
Nimmo, F., Spencer, J.R., Pappalardo, R.T., Mullen, M.E., 2007. Shear heating as the origin of the plumes and heat flux on Enceladus. Nature 447 (7142), 289–291.
Osinski, G.R., Pierazzo, E. (Eds.), 2013. Impact Cratering Processes and Products. Wiley-Blackwell.
Pappalardo, R.T., Belton, M.J.S., Breneman, H.H., Carr, M.H., Chapman, C.R., Collins, G. C., Denk, T., Fagents, S., Geissler, P.E., Giese, B., Greeley, R., Greenberg, R., Head, J. W., Helfenstein, P., Hoppa, G., Kadel, S.D., Klaasen, K.P., Klemaszewski, J.E., Magee, K., McEwen, A.S., Moore, J.M., Moore, W.B., Ryan, E.V., Davies, D.R., Giblin, I., 1999. A laboratory impact study of simulated Edgeworth–Kuiper Belt objects. Icarus 142, 52–62.
Pierazzo, E., Melosh, H.J., 2000. Understanding oblique impacts from experiments, observations and modelling. Annu. Rev. Earth Planet. Sci. 28, 141–167.
Ryan, E.V., Davies, D.R., Giblin, I., 1999. A Laboratory Impact Study of Simulated EdgeworthKuiper Belt Objects. Icarus 142, 52–62.
Sohl, F., Choukroun, M., Kargel, J., Kimura, J., Pappalardo, R., Vance, S., Zolotov, M., 2010. Subsurface water oceans on icy satellites: chemical composition and exchange processes. Space Sci. Rev. 153, 485–510.
Sonett, C.P., Pearce, S.J., Gault, D.E., 1991. The oceanic impact of large objects. Adv. Space Res. 1196, 77–86.
Sparks, W.B., Hand, K.P., McGrath, M.A., Bergeron, E., Cracraft, M., Deustua, S.E., 2016. Probing for evidence of plumes on Europa with HST/STIS. Astrophys. J. 829, 121 (21 pages).
Thomas, P.C., Burns, J.A., Helfenstein, P., Squyres, S., Veverka, J., Porco, C., Turtle, E.P., McEwen, A., Denk, T., Giese, B., Roatsch, T., Johnson, T.V., Jacobson, R.A., 2007. Shapes of the Saturnian icy satellites and their significance. Icarus 190, 573–584.
Thomas, P.C., Tajeddine, R., Tiscareno, M.S., Burns, J.A., Joseph, J., Loredo, T.J., Helfenstein, P., Porco, C., 2016. Enceladus's measured physical libration requires a global subsurface ocean. Icarus 264, 37–47.
Turtle, E.P., Pierazzo, E., 2001. Thickness of a Europan ice shell from impact crater simulations. Science 294 (5545), 1326–1328.
Waite, J.H., Combi, M.R., Ip, W.H., Cravens, T.E., McNutt, R.L., Kasprzak, W., Yelle, R., Luhmann, J., Niemann, H., Gell, D., Magee, B., Fletcher, G., Lunine, J., Tseng, W.L., 2006. Cassini ion and neutral mass spectrometer: Enceladus plume composition and structure. Science 311 (5766), 1419–1422.
Zahnle, K., Schenk, P., Levison, H., Dones, L., 2003. Cratering rates in the outer Solar System. Icarus 163, 263–289.